Supporting Information:

A high effective and stable $CuZn_{0.3}Mg_xAlO_y$ catalyst for the manufacture of chiral L-phenylalaninol: The role of Mg and its hydrotalcite-like precursor

Zhangping Shi,[a] Shuangshuang Zhang,[a] Xiuzheng Xiao,[a] Dongsen Mao[a] and Guanzhong Lu[ab]*

[a] Research Institute of Applied Catalysis, School of Chemical and Environmental Engineering, Shanghai Institute of Technology, Shanghai 201418, China.

[b] Key Laboratory for Advanced Materials and Research Institute of Industrial catalysis, East China University of Science and Technology, Shanghai 200237, China.

*Corresponding Author: Fax: +86-21-64252923. E-mail: gzhlu@ecust.edu.cn (G.Z. Lu).

1. Structural and textural properties of the CZA-0 catalyst

The structural properties and pore size distribution curves of the unreduced, fresh and deactivated CZA-0 catalyst are shown in Table S1 and Fig. S1. The results show that no significant difference between the unreduced and fresh catalyst can be found, indicating that the structural properties and pore size distribution of the CZA-0 catalyst are hardly affected by H_2 during the reduction. After deactivation of CZA-0, its BET surface area, pore volume and mean pore size were slightly declined, and its micropores increased and the mesopores decreased, indicating that the pore channels in the deactivate catalyst were seriously blocked, resulting in the change of pore size distribution. Since the carbon deposition is not common on the copper catalysts for the liquid-phase reaction,[S1] the formation of polyamide by self-polymerization of L-Phenylalanine methyl ester during the reaction (Scheme S1), which are insoluble and thermostable, may block the pores of the CZA-0 catalyst, resulting in a decrease in the pore size and the deactivation of the CZA-0 catalyst by making the active sites inaccessible to the reactants.

Table S1. Structural and textural properties of $Cu/ZnO/Al_2O_3$ catalysts.

Catalyst	BET surface area (m^2/g)	Pore volume (cm^3/g)	Average pore diameter (nm)	Crystallite size of Cu^0 (nm) [a]
Unreduced	92	0.42	18.58	-
Fresh	85	0.40	17.85	13.0
Deactivated	74	0.33	15.46	16.6

[a] Cu metal crystallite size was determined by the Scherrer equation based on the XRD diffraction peak broadening.

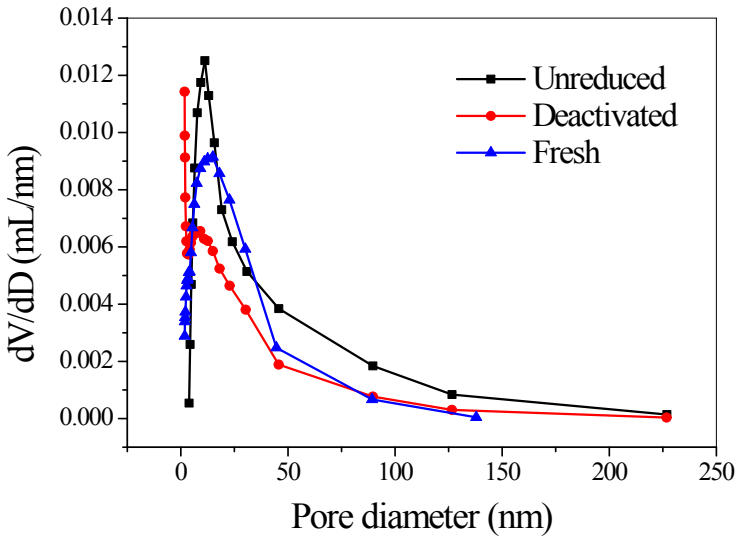

Fig. S1. Pore size distribution curves of the CZA-0 catalysts.

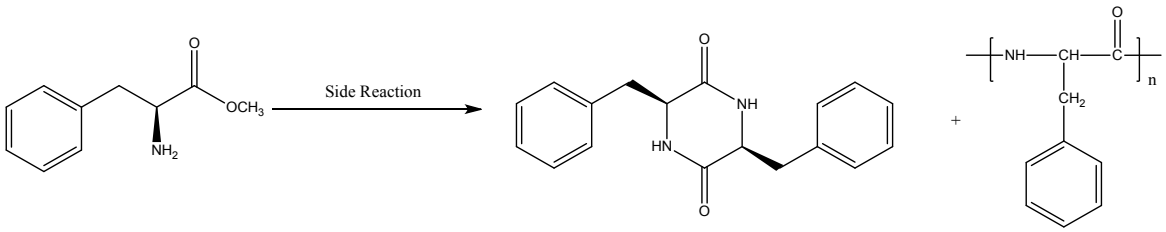

Scheme S1. The self-polymerization of L-Phenylalanine methyl ester.[S2]

Fig. S2 shows the XRD patterns of the fresh, deactivated and unreduced CZA-0 catalysts. No diffraction peaks of Al_2O_3 and ZnO can be detected in these catalysts, suggesting that the oxide species are amorphous and/or high-dispersed. Weak and board diffraction peaks of CuO phase (JCPDS 80-1268) appeared at $2\theta = 35.6°$, 38.8° in the unreduced catalyst. The characteristic peaks of spinel structure $ZnAl_2O_4$ phase (ICDD 5-669) are observed in the fresh and deactivated

catalysts, indicating that $ZnAl_2O_4$ phase can be formed after reduction by H_2. In the XRD pattern of the fresh catalyst, no diffraction peaks of Cu_2O and CuO can be detected, that is, CuO was completely reduced to metallic copper after reduction. The fact that the similar XRD patterns of fresh and deactivated catalysts, indicates that surface oxidation of metallic copper is not the cause of deactivation, but the characteristic peaks of metallic copper in the deactivated catalyst became sharper than that of the fresh sample, which suggests that the deactivated catalyst exhibits significant growth of Cu crystallites.

It was reported that the presence of chloride could accelerate the surface migration process of metallic copper and promote the growth of crystallite and catalyst agglomeration.[S1,S3] Hence, it can be speculated that the small amount of residual chloride ions during the preparation of L-Phenylalanine methyl ester would promote the growth of metallic copper crystallites, which is responsible for the decrease in the catalytic performance of the CZA-0 catalyst.

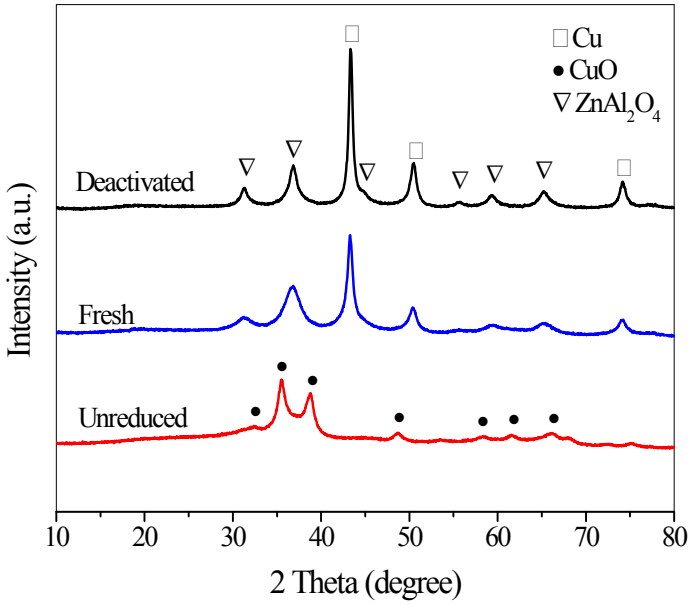

Fig. S2. XRD patterns of deactivated, fresh, and unreduced CZA-0 catalysts.

2. The morphology of the CZA-0 catalyst

The TEM images of the fresh and deactivated catalysts are in Fig. S3. It can be seen that the Cu^0 particles of the fresh catalyst are of uniform distribution and its size is 4−8 nm. For the deactivated sample, the agglomeration of Cu^0 particles could be observed and its average grain

size was above 15 nm. These results are in good agreement with the crystallite size of Cu^0 calculated from XRD patterns.

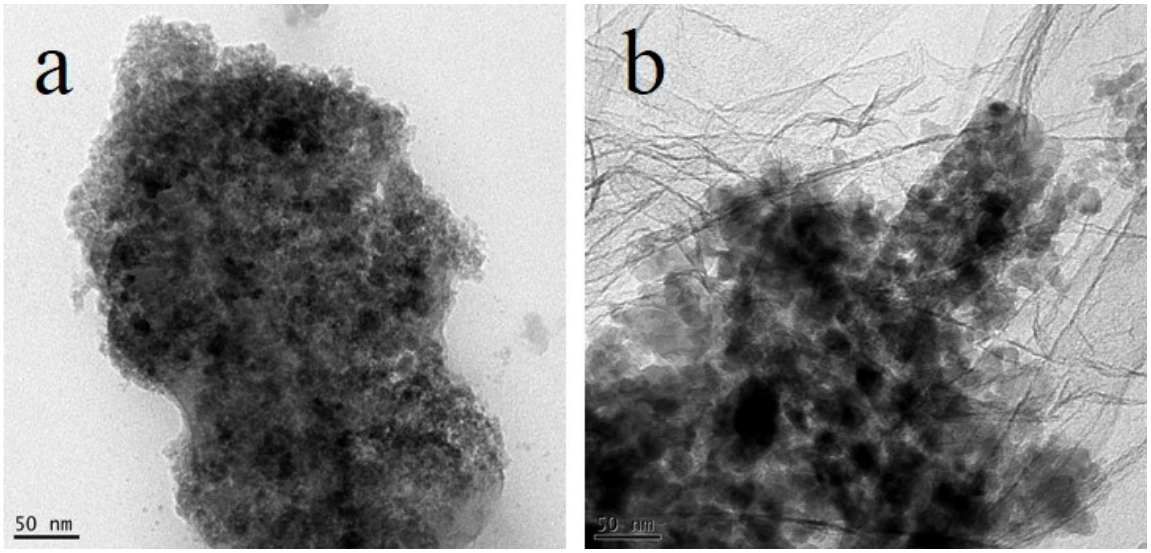

Fig. S3. TEM images of (a) fresh and (b) deactivated catalysts.

3. The surface composition of the CZA-0 catalyst.

The XPS spectra of fresh and deactivated CZA-0 catalysts are shown in Fig. S4 and their surface compositions are listed in Table S2. Before the XPS measurement, the deactivated catalyst was pretreated with the ultrasonic washing using ethanol three times, and then was dried in a vacuum oven. As shown in Fig. S4, the transition peaks of C 1s and N 1s were located at 282.7 and 397.4 eV, and for the deactivated catalyst, the peak areas of C 1s and N 1s are much larger than that of the fresh sample. As shown in Table S2, the surface concentration of C and N were increased obviously after CZA-0 was used in the reaction, which shows that some compounds containing the N and C elements was formed on the catalyst surface and should be the insoluble polyamide. As the formed polyamide covered on the catalyst surface, the relative surface concentration Cu and ZnO species lowered comparing with the fresh catalyst, resulting in the obvious decrease in surface area, pore volume and average pore size for the deactivated catalyst.

The XPS peaks of Cu $2p_{1/2}$ and Cu $2p_{2/3}$ could be deconvoluted into two peaks. The Cu 2p peaks located at BE = 932.2 and 952.3 eV for the fresh sample (or 931.7 and 951.8 eV for the deactivated sample) are the characteristic XPS peaks of Cu^{2+} species.[S4,S5] In addition, the

presence of the satellite peak at ~942 eV showed also this Cu^{2+} ion from $ZnAl_2O_4$ [S4,S6], which is in good agreement the results of XRD. The Cu 2p peaks at 930.2 and 950.2 eV for the fresh sample (or 929.7 and 949.7 eV for the deactivated sample) are the characteristic peaks of metallic copper or Cu_2O, because the binding energy of metallic copper almost be the same as that of Cu_2O.[S6]

Comparing with the fresh CZA-0 catalyst, the Cu 2p peaks of the deactivated catalyst shifted to the lower binding energy of ~0.5 eV, which is attributed to the presence of N atoms on the deactivated sample. The electron-donating effect of N atoms makes the transition of inner electrons in Cu atom easier than that of the fresh catalyst, resulting in the reduction of the binding energy of the Cu 2p orbit.

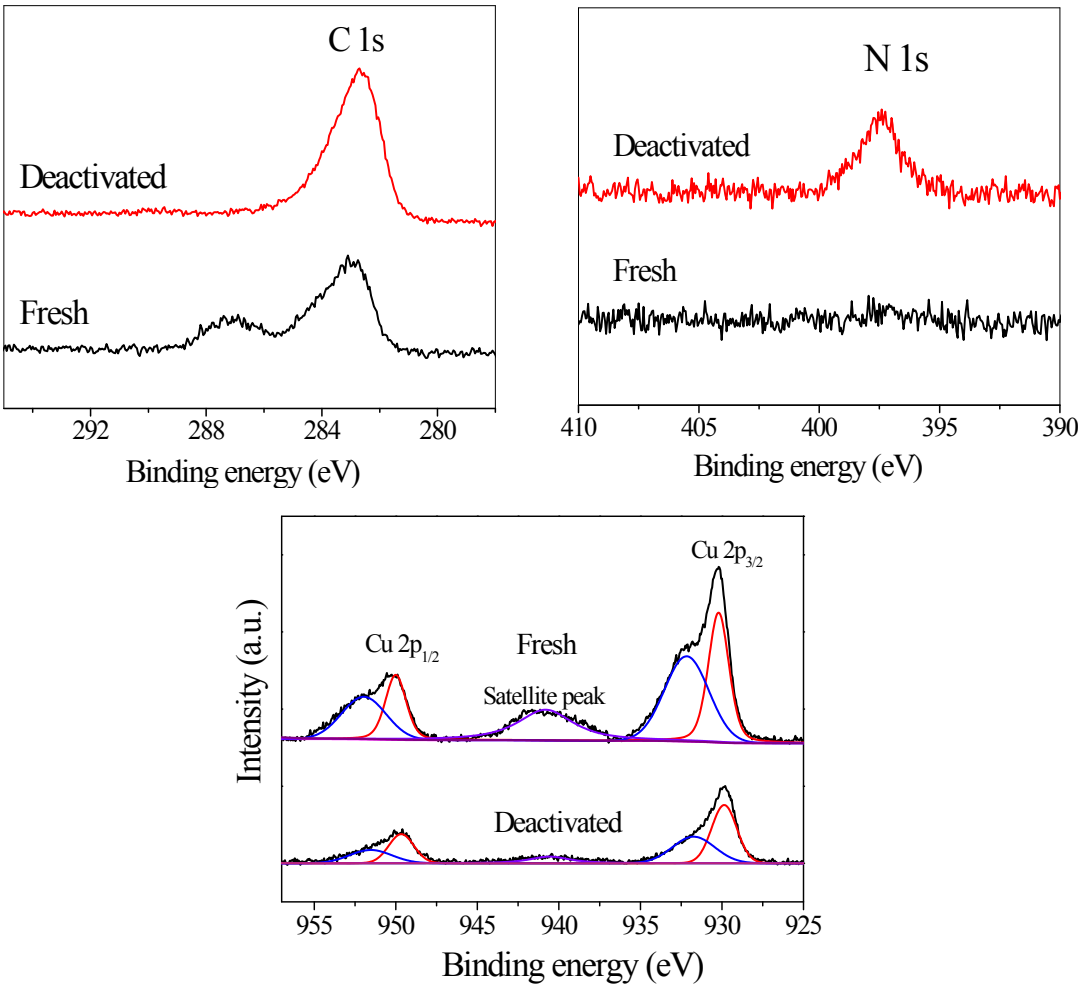

Fig. S4. XPS spectra of the fresh and deactivated CZA-0 sample.

Table S2. Binding energy data of surface elements and their surface composition on the CZA-0 catalysts obtained by XPS spectra.

	Binding energy (eV) Fresh (Deactivated)	Surface concentration (%)	
		Fresh (Deactivated) (Mass%)	Fresh (Deactivated) (Atom%)
Cu 2p	930.2 (929.8) *	28.02 (19.13)	9.9 (5.88)
Zn 2p	1019.55 (1018.95)	13.31 (14.44)	4.57 (4.31)
C 1s	283.1 (282.7)	10.49 (21.59)	19.61 (35.11)
N 1s	397.95 (397.4)	0.15 (2.67)	0.24 (3.73)
O 1s	529.05 (528.5)	44.02 (40.85)	61.76 (49.76)

* The values in parentheses from the deactivated catalysts.

4. TG-DTG curves of the deactivated catalyst

Fig. S5 showed the TG-DTG curves of the deactivated catalyst, which was conducted in N_2 flow at 10 °C/min. The weight loss at < 150 °C should be related to desorption of some low boiling compounds adsorbed on the catalyst, such as water, methanol and ethanol. The weight loss at 150−310 °C can be attributed to desorption of the reactants and product adsorbed on the catalyst, such as, L-phenylalanine methyl ester and L-phenylalaninol. The weight loss at > 310 °C should be ascribed to the decomposition of the formed polyamide, because of its high melting point and temperature resistance.[S7] Therefore, it can be concluded that the polyamide accumulated on the surface and channels of the catalyst made the CZA-0 catalyst deactivate.

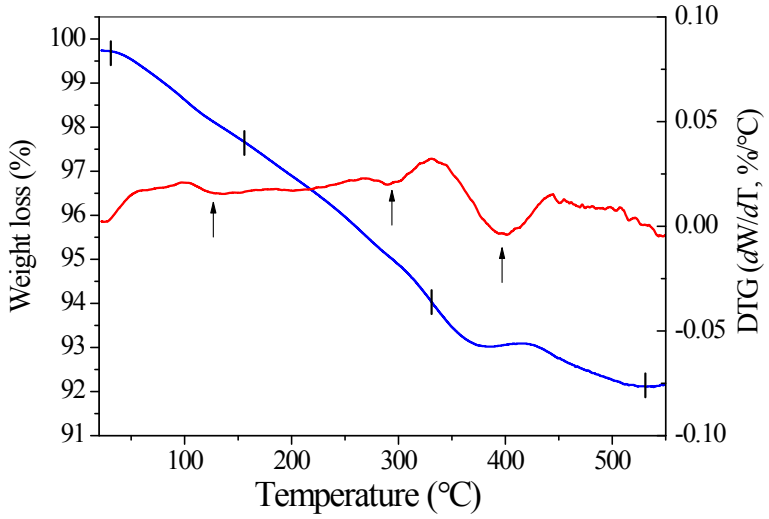

Fig. S5. TG-DTG curves of the deactivated CZA-0 catalyst.

5. Regeneration of the deactivated catalyst

Based on results discussed above, the blockage by polyamide is another important cause of the deactivation of the CZA-0 catalyst except the growth of metallic copper crystallites. Hence, the regeneration process for the deactivated CZA-0 catalyst was designed to be the treatment of oxidation – reduction, in which the deactivated catalyst was calcined in air at 450 °C for 4 h and then reduced by H_2 under a pressure of 1 MPa at 250 °C for 4 h in the stainless steel autoclave. After that, the catalytic performance of the deactivated CZA-0 catalyst can be recovered to some extent, for instance, using this regenerated CZA-0 catalyst, the conversion of L-phenylalanine methyl ester of 96.7% and the yield of L-phenylalaninol of 78.4 % could obtained.

References

[S1] Twigg, M. V.; Spencer, M. S., Deactivation of supported copper metal catalysts for hydrogenation reactions. *Applied Catalysis A: General* **2001,** *212* (1), 161-174.

[S2] Usuki, H.; Yamamoto, Y.; Arima, J.; Iwabuchi, M.; Miyoshi, S.; Nitoda, T.; Hatanaka, T., Peptide bond formation by aminolysin-A catalysis: A simple approach to enzymatic synthesis of diverse short oligopeptides and biologically active puromycins. *Organic & Biomolecular Chemistry* 2011, 9 (7), 2327-2335.

[S3] Huang, H.; Wang, S.; Wang, S.; Cao, G., Deactivation mechanism of Cu/Zn catalyst poisoned by organic chlorides in hydrogenation of fatty methyl ester to fatty alcohol. *Catalysis letters* **2010,** *134* (3-4), 351-357.

[S4] He, L.; Cheng, H.; Liang, G.; Yu, Y.; Zhao, F., Effect of structure of $CuO/ZnO/Al_2O_3$ composites on catalytic performance for hydrogenation of fatty acid ester. *Applied Catalysis A: General* **2013,** *452* (1), 88-93.

[S5] Agrell, J.; Birgersson, H.; Boutonnet, M.; Melián-Cabrera, I.; Navarro, R.; Fierro, J. G., Production of hydrogen from methanol over Cu/ZnO catalysts promoted by ZrO_2 and Al_2O_3. *Journal of Catalysis* **2003,** *219* (2), 389-403.

[S6] Chen, L.-F.; Guo, P.-J.; Qiao, M.-H.; Yan, S.-R.; Li, H.-X.; Shen, W.; Xu, H.-L.; Fan, K.-N., Cu/SiO_2 catalysts prepared by the ammonia-evaporation method: Texture, structure, and catalytic performance in hydrogenation of dimethyl oxalate to ethylene glycol. *Journal of Catalysis* **2008,** *257* (1), 172-180.

[S7] Li-Hua, Q.; Zong-Xuan, S.; Wu-Hong, C.; Yong, Z.; Ya-Wen, Z., A Convenient Approach to the Enantiopure (15, 25, 45, 55)- and (1R, 2S, 4R, 5S)-2, 5- Bis (phenylmethyl)- l, 4- diazabicyclo [2, 2, 2]- octane. *Chinese Journal of Chemistry* 2003, 21 (8), 1098-1100.